IEEE Access
Multidisciplinary | Rapid Review | Open Access Journal

Received October 17, 2021, accepted October 28, 2021, date of publication November 15, 2021, date of current version November 18, 2021.

Digital Object Identifier 10.1109/ACCESS.2021.3125458

High-Efficiency Dielectric Reflectarray Antennas With Ultra-Wideband Characteristics

EUN-CHEOL CHOI AND SANGWOOK NAM, (Senior Member, IEEE)
School of Electrical and Computer Engineering, Institute of New Media Communication, Seoul National University, Seoul 08826, South Korea

Corresponding author: Sangwook Nam (snam@snu.ac.kr)

This work was supported in part by the Center for Advanced Meta-Material by the Ministry of Science, ICT and Future Planning as Global Frontier Project under Grant CAMM-2014M3A6B3063708.

ABSTRACT In this study, a K-band offset dielectric reflectarray antenna, having high aperture efficiency and ultra-wideband characteristics, was designed. A column-type dielectric unit cell was employed for the dielectric reflectarray elements. To obtain the ultra-wideband characteristics, an effective arrangement of the dielectric elements was implemented by considering the relative phase requirement. In addition, the real phase error and element patterns were calculated and analyzed using the equivalence principle and full-wave simulations. The prototype of the dielectric reflectarray antenna was fabricated by milling a dielectric sheet. The performance of the proposed antenna was measured and observed to be in good agreement with the simulation results. The measured results demonstrate that the maximum aperture efficiency was 63% at 22 GHz and bandwidth for an aperture efficiency exceeding 40% was 42.5%. The achieved results signified the importance of the arrangement strategy of the elements to achieve better efficiency and wider bandwidth performances.

INDEX TERMS Dielectric antennas, millimeter wave, reflectarray, relative phase error, wideband.

I. INTRODUCTION

A reflectarray antenna combines the advantages of a parabolic reflector antenna and phased-array antenna [1]. Based on geometrical optics, the parabolic reflector antenna compensates for the phase delays of the different paths from the feed horn through the curved surface [2]. Therefore, the gain performance increases with frequency due to the effective increment in the electrical size of the reflector surface. However, it is expensive and difficult to manufacture owing to its specifically curved surface.

The reflectarray antenna could achieve a high gain performance because the radiating elements compensate for the spatial phase delay from the feed horn at any target frequency. However, when the frequency changes the gain of the reflectarray could significantly deteriorate. This bandwidth limitation is caused by two different factors viz., the narrow band of the radiating elements and the differential spatial phase delay according to the different paths from the feed horn to each position of the array surface [3]–[5]. Therefore, various unit-cell structures have been used to obtain wideband characteristics [6]–[8]. In these cases, wide-gain bandwidth was achieved by improving the parallel slope of the reflection phase with reference to the frequency variation rather than the S-shape reflection phase response. However, phase compensation could not be implemented effectively within an ultra-wide bandwidth because the larger the change in the frequency the higher the differential spatial phase delay. Thus, the 1 -dB gain bandwidth of the conventional wideband reflectarray antennas was limited to 25−35% approximately [6], [9], [10].

In this study, to effectively compensate for the differential spatial phase delay, within an ultra-wide bandwidth, the desired reflection phase response with reference to the frequency variation was investigated by considering the relative phase requirement and the appropriate phase slope of the unit cell was obtained using at column-type dielectric element. Dielectric reflectarray antennas have been proposed using various structures such as the dielectric resonant antenna (DRA), perforated dielectric reflectarray antennas, and column-type dielectric reflectarray antennas [11]–[18]. In DRA, the fabrication process of placing and bonding elements in the exact position is complicated and cumbersome [11], [12]. In perforated dielectric reflectarray antennas, the reflection phase was derived upon adjusting the effective dielectric constant by varying the number and

The associate editor coordinating the review of this manuscript and approving it for publication was Chun-Hsing Li.

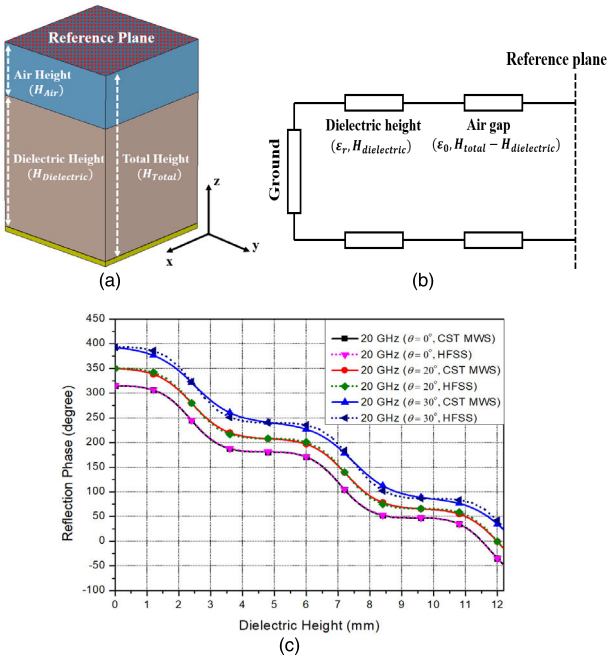

FIGURE 1. Dielectric column-type unit cell (H_{total} = 12.2mm). (a) Geometry of the dielectric unit cell, (b) equivalent transmission line model of the dielectric unit cell, (c) reflection phase ψ_i of the dielectric unit cell with reference to the incident angle for TM mode.

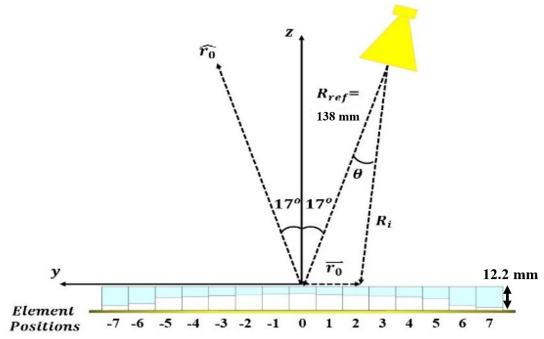

FIGURE 2. 2D-structural dimension of the dielectric reflectarray antenna for $\phi = 90°$.

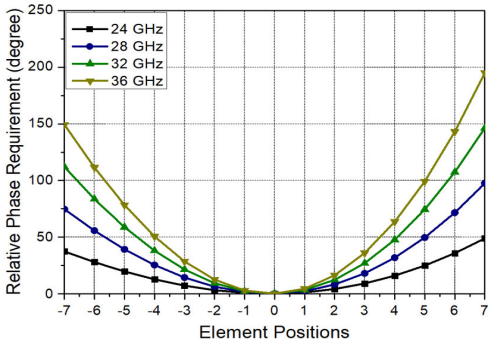

FIGURE 3. Relative phase requirement with reference to frequency variation for $\phi = 90°$.

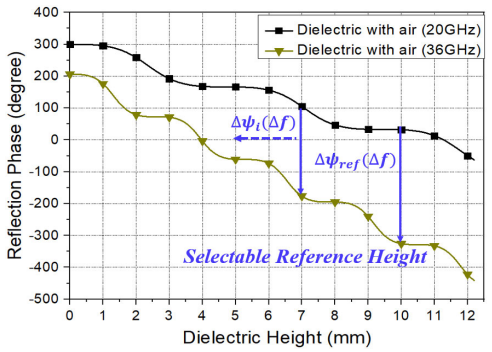

FIGURE 4. Reflection phase of the dielectric unit cell for normal incidence at different frequencies.

radius of the holes in the dielectric unit cell. However, to obtain wide bandwidth performance, multiple dielectric layers were required [14]–[16]. In column-type dielectric reflectarray antennas, the reflection phase was simply derived by adjusting the height of the dielectric. However, the previous column-type dielectric reflectarray antennas have disadvantages such as the fabrication tolerances, alignment errors, the loss and uncertainty of materials in the fabrication process using 3D printing [17], [18]. Therefore, the bandwidth and aperture efficiency performance of previous dielectric reflectarray antennas were less than 25 and 50%, respectively.

Thus, our aim was to achieve high-aperture efficiency and an ultra-wide bandwidth performance through an effective arrangement of the dielectric elements, taking into consideration the relationship between the differential spatial phase delay and frequency variation. In addition, to reduce fabrication errors, the dielectric sheets were milled using materials having low losses and displaying excellent machinability even at high frequencies.

II. DIELECTRIC UNIT CELL AND ANALYSIS OF RELATIVE PHASE ERROR

A. COLUMN-TYPE DIELECTRIC ELEMENTS FOR REFLECTARRAYS

The reflection phase of the column-type dielectric unit cell could be calculated using the short-ended transmission line model of the grounded dielectric slab with an air layer [19]. Figure 1 shows the geometry, equivalent model, and reflection phase of the dielectric unit cell. The dielectric material used in this study was Eccostock® 0005, manufactured by Laird Technology, with the following characteristics: relative permittivity $\varepsilon_r = 2.53$, and loss tangent $\tan\delta = 0.0005$ (1 MHz to 500 GHz) [20]. The reference frequency and periodicity of the unit cell is 20 GHz and 7.5mm, i.e., $1/2\lambda_0$, respectively. As the reflectarray antenna should satisfy the desired phase distribution on a reference plane, a reference plane of the dielectric element was setup with an air layer above the dielectric plane as shown in Fig. 1 (a) and (b). To verify the performance of unit cell elements, the measurements technique using the rectangular waveguide were implemented [21], [22]. However, in this paper, the measurement

of dielectric unit cell elements was substituted for unit cell simulation of CST MWS and HFSS. Figure 1 (c) shows the reflection phase of the dielectric unit cell with reference to the dielectric height variation. To satisfy the reflection phase of a full phase-cycle (360°), the maximum height of the dielectric element was set as 12.2mm.

B. RELATIVE PHASE ERROR AND ARRANGEMENT METHOD OF DIELECTRIC UNIT CELL

Figure 2 shows the cross-sectional view of the proposed reflectarray antenna for $\phi = 90°$. An offset feeding structure was selected to reduce the blockage effect, and a feed horn was used as the pyramidal horn antenna. The aperture dimensions and gain performance of the pyramidal feed horn are 28 mm × 24 mm and 15 dBi at 20 GHz, respectively. The offset angle is 17° and the distance from the phase center of the feeding horn to the center of the array surface is $R_{ref} =$ 138 mm. To effectively arrange the array elements on the aperture surface, the relationship between the geometry of the reflectarray structure and reflection phase characteristics of the unit cell was analyzed [23]. The relative phase error with respect to the frequency variation is represented as follows.

$$\begin{aligned} PE_i(f) &= \left|\left\{\psi_i(f) - \psi_{i,required}(f)\right\}\right. \\ &\quad \left. - \left\{\psi_{ref}(f) - \psi_{ref,required}(f)\right\}\right| \\ &\cong \left|\left\{(k-k_0)\left(-R_{ref} + R_i - \vec{r_i}\cdot\hat{r_0}\right)\right\}\right. \\ &\quad \left. + \left\{\Delta\psi_{ref}(\Delta f) - \Delta\psi_i(\Delta f)\right\}\right| \end{aligned} \quad (1)$$

where k_0 and k are the free-space wavenumbers at frequencies f_0 and f, respectively. As shown in Fig. 2, R_i is the distance between the phase center of the feed horn and the i-th element, $\vec{r}_i$ is the position vector of the i-th element, and $\hat{r}_0$ is the unit vector along the main beam direction. The element in the central position of the reflector surface was set as the reference element of reflectarray elements. Variables ψ_{ref} and $\psi_{ref,required}$ represent the reflection phase and required phase of the reference element, respectively, while ψ_i and $\psi_{i,required}$ represent the reflection phase and required phase of the i-th outer position elements from the reference position, respectively. Variables $\Delta\psi_{ref}(\Delta f)$ and $\Delta\psi_i(\Delta f)$ indicate the reflection phase shift of the central and outer position elements, respectively, with reference to frequency variation. To achieve wideband performance, an appropriate phase compensation was implemented by considering the two terms of the relative phase error. Figure 3 shows the relative phase requirement $(k - k_0)\left(-R_{ref} + R_i - \vec{r}_i \cdot \hat{r}_0\right)$ for the compensation of the geometric phase change with respect to different frequencies. The relative phase requirement increases gradually from the central to the outer position of the array surface. To reduce (1), the reflection phase shift difference, expressed as $\Delta\psi_{ref}(\Delta f) - \Delta\psi_i(\Delta f)$, need to be gradually decreased from the central to the outer positions of the reference surface. These characteristics were realized when the phase shift quantity $\left|\Delta\psi_i(\Delta f)\right|$ of the i-th elements were gradually decreased from the central to the outer positions, as shown in Fig. 4, where the reflection phase of the

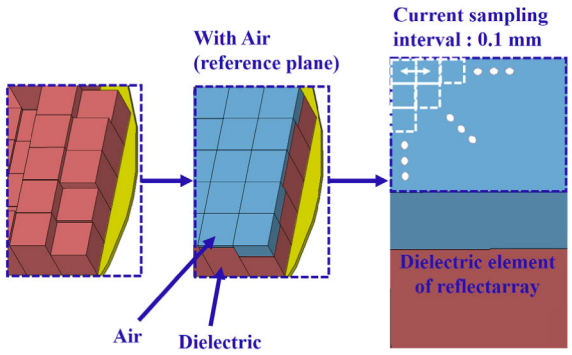

FIGURE 5. Setting the current sampling on the reference plane of the dielectric reflectarray elements to calculate the real element characteristics.

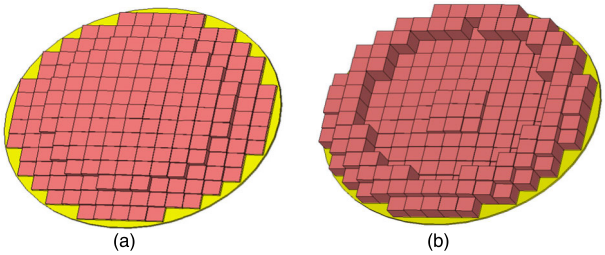

FIGURE 6. Dielectric reflectarray surface according to the different heights of the reference element. (a) $H_{ref} = 8.7mm$, (b) $H_{ref} = 6.0mm$.

dielectric unit cell is shown with respect to height variation at frequencies of 20 and 36 GHz. As shown in Fig. 4, when the reference element with a greater dielectric height was selected and the dielectric height of the outer elements was lower, progressively according to the distance from the element in the center, the reflection phase shift difference decreased gradually from the central position toward the outer positions. This resulted in an effective compensation of the geometric phase change. Thus, arrangement of the dielectric elements without the phase-wrapped sections (dielectric height jumping from a maximum to minimum, or vice versa) should be implemented because when phase wrapping occurred, the height of the outer element was greater than that of the reference element, resulting in distortion of the phase compensation.

III. REAL RELATIVE PHASE ERROR AND RADIATION PATTERNS OF DIELECTRIC ELEMENTS

To evaluate the characteristics of the reflectarray antenna structure, we calculated the real relative phase error and element patterns of the reflectarray antennas by the vector potential integral of the equivalent current sources based on the equivalence principle and full-wave simulations [24]. Figure 5 shows the equivalent current source sampling on the reference plane of the dielectric reflectarray elements. Based on the equivalence principle, the equivalent electric and magnetic current sources can be obtained by the tangential magnetic and electric field components, respectively [2]. The tangential magnetic and electric field components were obtained at intervals of 0.1mm using full-wave simulations

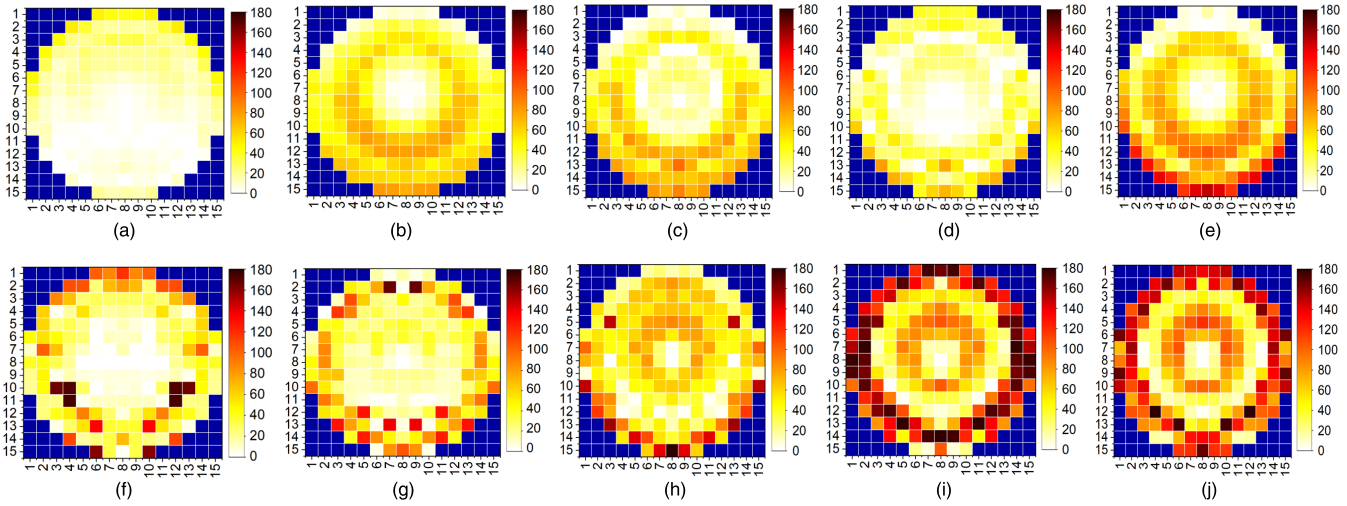

FIGURE 7. Real relative phase error of the dielectric reflectarray based on the equivalence principle and full-wave simulation. (a) $H_{ref} = 8.7mm$ at 20 GHz, (b) 24 GHz, (c) 28 GHz, (d) 32 GHz, (e) 36 GHz; (f) $H_{ref} = 6.0mm$ at 20 GHz, (g) 24 GHz, (h) 28 GHz, (i) 32 GHz, (j) 36 GHz.

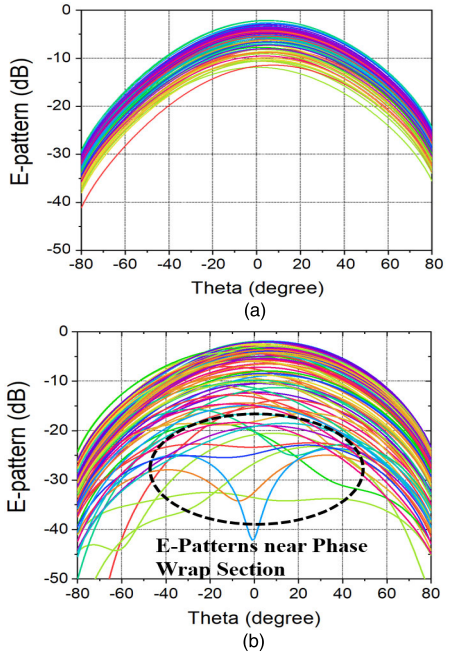

FIGURE 8. Real element patterns of the dielectric reflectarray based on the equivalence principle and full-wave simulations at the reference frequency of 20 GHz. (a) $H_{ref} = 8.7mm$, (b) $H_{ref} = 6.0mm$.

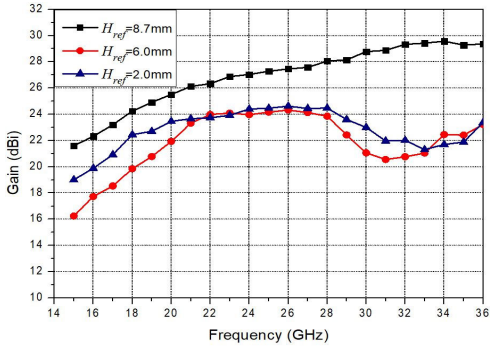

FIGURE 9. Simulated gain characteristics according to the different heights of the reference element.

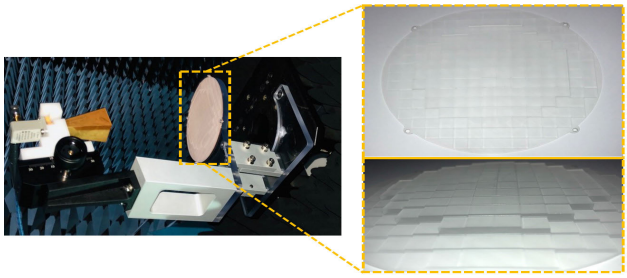

FIGURE 10. Fabricated prototype of the proposed dielectric reflectarray antenna of $H_{ref} = 8.7mm$. (a) Prototype of the dielectric reflectarray antenna, (b) top and side view of the dielectric reflectarray aperture.

of the dielectric reflectarray antenna. Thus, the equivalent current sources on the reference plane of the dielectric element, having a layer of air, were obtained at intervals of 0.1 mm. Particularly, for a dielectric element of 7.5 mm ($\lambda/2$), equivalent current sources of 5625 points were obtained. Figure 6 (a) and (b) represent the dielectric reflectarray surface with reference to the choice of heights of the reference element of 8.7 mm and 6 mm, respectively. As shown in Fig. 6 (a), the phase-wrapped section did not occur from the center toward the outer elements. However, in the case of H_{ref} = 6mm, phase-wrapped sections occurred in the outer elements, resulting in a significant degradation of the relative phase error. Figure 7 represents the real relative phase errors with respect to the choice of different heights of the reference dielectric elements at different frequencies. The real relative phase error was defined by the real phase error of the reflectarray elements with respect to the central element, and calculated based on the potential integral of the equivalent current sources [23]. In the case of H_{ref} = 8.7 mm, although the phase error increased slightly as the frequency

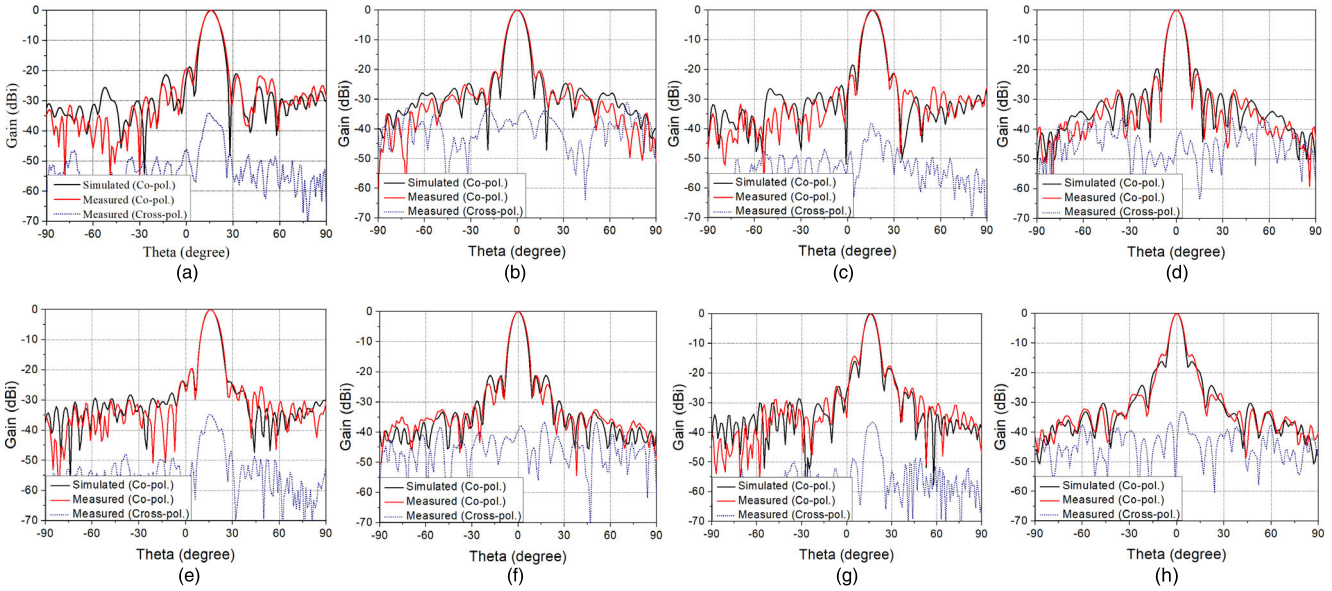

FIGURE 11. Simulated and measured radiation patterns on the (a) E-plane and (b) H-plane at 18 GHz; (c) E-plane and (d) H-plane at 20 GHz; (e) E-plane and (f) H-plane at 24 GHz; and (g) E-plane and (h) H-plane at 26 GHz.

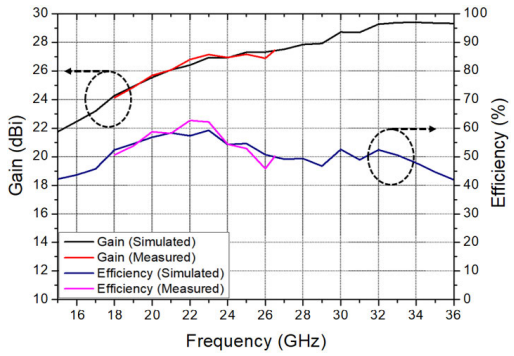

FIGURE 12. Simulated and measured gain and corresponding aperture efficiency.

TABLE 1. Comparison with previous dielectric reflectarray antennas.

	Type	Freq. / GHz	Size / λ_0	F/D	Max. Effi. / %	1-dB Gain BW. / %	>40% Effi. BW. / %
This work	Column	20	8	1.15	63	N. A.[4]	105[1] 42.5[3]
[11]	DRA	9	8.7	1.27	60	8	
[17]	Column	100	10	0.75	23.4[1] 14.2[2]	20.7	
[15]	Perforated	30	8.2	1.145	38	6	
[14]	Perforated	13.5	13.5	0.8	45.6	18.1	22.8
[25]	DRA	30	12	1.12	31	12	
[26]	DRA	35	14	0.85	17.7	23	
[18]	Column	220	20.5	2.75	27.6[1] 10.3[2]	20.9	
[16]	Perforated	73.5	19.6	0.9	41.89	6.8	1.4

1): Simulated performance, 2): Measured performance, 3): Measured performance from 18 to 26.5 GHz, 4) Not applicable.

increased, the overall relative phase errors were extremely low. However, in the case of H_{ref} = 6mm, the relative phase errors increased significantly as the frequency increased. Moreover, at the 6th to 7th element positions, the phase error significantly deteriorated at the section where phase wrapping occurred. Figure 8 shows the real radiation characteristics of each dielectric element in the reflectarray at a center frequency of 20 GHz. The real radiation characteristics were calculated based on the potential integral of the equivalent current sources. As shown in Fig. 8 (a), the element patterns of H_{ref} = 8.7 mm were not distorted. In contrast, in the case of the H_{ref} = 6 mm, the element patterns of a large number of the dielectric elements were significantly distorted. It was observed that in the reference plane of curtain dielectric elements the equivalent current distribution on the reference plane was altered by the scattering effects, which was due to the occurrence of phase wrapping in the dielectric elements with greater heights. Figure 9 represents the simulated gain performance according to the choice of height of the reference element. In the case of H_{ref} = 8.7mm, the gain performance increased as the frequency increased because phase compensation was appropriately implemented. In contrast, for H_{ref} = 6mm, the gain performance at the center frequency of 20 GHz was low and the gain performance significantly deteriorated after 28 GHz. In addition, to show the performance of the reference material with additional height, having phase wrapped sections on the aperture surface, the gain performance for H_{ref} = 2 mm was included. It was observed that the gain performance deteriorated as the frequency varied, similar to that observed in the case of H_{ref} = 6 mm. Moreover, it was noted that the relative phase error and effect of scattering increased due to the occurrence of phase wrapping. Therefore, to achieve high efficiency and wide bandwidth performance, the reference dielectric element should be selected such that the phase wrapping does not occur over the entire aperture surface.

IV. EXPERIMENTAL RESULTS

A K-band dielectric reflectarray antenna was designed and fabricated. The height of the reference element of the proposed antenna was selected as 8.7 mm, according to the analysis in Sections II and III. Figure 10 shows the prototype of the proposed antenna and the measurement environment. The proposed dielectric reflectarray antenna was fabricated by milling the Eccostock® 0005 substrate sheet with a machining tolerance of 0.05 mm. The reference frequency of the proposed antenna was 20 GHz. The diameter of the aperture surface was 120 mm, i.e., $8\lambda_0$; the focal length was 138 mm, and the focus to diameter (F/D) ratio was 1.15. Figure 11 shows the radiation patterns in the E- and H-planes at different frequencies. Although the simulated gain bandwidth of the designed antenna satisfied the Ku-, K-, and Ka-bands, the gain performance of the designed antenna was measured only at the K-band frequencies, due to the limitation of cutoff frequency of the fabricated feed horn. The measured radiation patterns were in agreement with the simulated results in the target bandwidth. The cross-polarization components were below −30 dB. The side lobe levels (SLL) of the measured results were observed to be approximately −20 dB from 18 to 24 GHz. However, at 26 GHz, the SLL was approximately −15 dB. It is expected that as the frequency increases from the reference frequency of 20 GHz, the phase errors gradually increase as shown in Fig. 7.

In general, the bandwidth of reflectarray antennas has been defined as the 1-dB gain bandwidth. This figure of merit has been selected because the gain performance of conventional reflectarray antennas deteriorate significantly with frequency variation. Because the proposed reflectarray antenna showed increasing gain characteristics with increasing frequency, owing to the proposed phase compensation method, evaluating the bandwidth performance based on gain reduction was not the appropriate method. An alternative approach to evaluate the bandwidth performance, based on aperture efficiency, has been described and defined in [7], [27], [28]. Such an approach was adopted in this study, and the bandwidth was defined as that which satisfies an efficiency exceeding 40%. Figure 12 shows the gain and efficiency performance with respect to frequency variation. The measured aperture efficiencies were calculated by the measured gain performances as follows.

$$\eta_{aperture\ efficiency} = \lambda^2 G_{measured} \Big/ 4\pi A \tag{2}$$

where $G_{measured}$ and A are the measured gain performances and physical area of reflectarray antenna, respectively. λ is wavelength according to different frequencies. The measured gain performances were in agreement with the simulated results within the K-band, and a maximum efficiency of 63% was achieved at 22 GHz. The simulated and measured bandwidths, for an aperture efficiency exceeding 40%, were in the ratio of 2.4:1 (15 − 36 GHz) and 1.47:1 (18 − 26.5 GHz), respectively. Table 1 shows a comparison of the results obtained for the various dielectric reflectarray antennas studied previously. In addition, the bandwidth performances observed in earlier studies were below 21%, which is significantly low as compared to our proposed dielectric reflectarray antenna. Thus, the dielectric reflectarray antenna proposed herein demonstrated substantially better efficiency and bandwidth performance than those reported on in previous studies. Moreover, even if the large aperture size or small F/D values of proposed dielectric reflectarray antenna are selected, the improved performances can be obtained considering an effective arrangement strategy without the phase-wrapped sections.

V. CONCLUSION

To achieve ultra-wideband characteristics, the optimal height of the reference element was studied and analyzed in this study, taking into consideration the relative phase requirement and reflection phase characteristics of the column-type dielectric unit cell. Further, to evaluate the characteristics of the proposed dielectric reflectarray, the real phase error and element patterns were calculated and analyzed using the equivalence principle and the full-wave simulation. It was observed that the arrangement of the dielectric elements implemented herein, which prevented the occurrence of phase wrapping, could effectively minimize the relative phase error and eliminate pattern distortion. The proposed reflectarray antenna demonstrated superior efficiency and bandwidth performance as compared to those reported on in previous research. The characteristics of the fabricated antenna were measured in the frequency range of 18−26.5 GHz, and the measured results were observed to be in good agreement with the simulation results.

REFERENCES

[1] D. M. Pozar, S. D. Targonski, and H. D. Syrigos, "Design of millimeter wave microstrip reflectarrays," *IEEE Trans. Antennas Propag.*, vol. 45, no. 2, pp. 287–296, Feb. 1997.
[2] C. A. Balanis, *Antenna Theory: Analysis and Design*. Hoboken, NJ, USA: Wiley, 2016.
[3] J. Huang and J. A. Encinar, *Reflectarray Antennas*. Piscataway, NJ, USA: IEEE Press, 2008.
[4] P. Nayeri, F. Yang, and A. Z. Elsherbeni, *Reflectarray Antennas: Theory, Designs and Applications*. Hoboken, NJ, USA: Wiley, 2018.
[5] J. Shaker, M. R. Chaharmir, and J. Ethier, *Reflectarray Antennas: Analysis, Design, Fabrication, and Measurement*. Norwood, MA, USA: Artech House, 2013.
[6] X. Xia, Q. Wu, H. Wang, C. Yu, and W. Hong, "Wideband millimeter-wave microstrip reflectarray using dual-resonance unit cells," *IEEE Antennas Wireless Propag. Lett.*, vol. 16, pp. 4–7, 2017.
[7] R. Deng, S. Xu, F. Yang, and M. Li, "A single-layer high-efficiency wideband reflectarray using hybrid design approach," *IEEE Antennas Wireless Propag. Lett.*, vol. 16, pp. 884–887, 2017.
[8] J. A. Encinar, "Design of two-layer printed reflectarrays using patches of variable size," *IEEE Trans. Antennas Propag.*, vol. 49, no. 10, pp. 1403–1410, Oct. 2001.
[9] J. H. Yoon, Y. J. Yoon, W. S. Lee, and J. H. So, "Broadband microstrip reflectarray with five parallel dipole elements," *IEEE Antennas Wireless Propag. Lett.*, vol. 14, pp. 1109–1112, 2015.
[10] L. Guo, H. Yu, W. Che, and W. Yang, "A broadband reflectarray antenna using single-layer rectangular patches embedded with inverted L-shaped slots," *IEEE Trans. Antennas Propag.*, vol. 67, no. 5, pp. 3132–3139, May 2019.
[11] F. Ahmadi, K. Forooraghi, Z. Atlasbaf, and B. Virdee, "Dual linear-polarized dielectric resonator reflectarray antenna," *IEEE Antennas Wireless Propag. Lett.*, vol. 12, pp. 635–638, 2013.

[12] M. G. N. Alsath, M. Kanagasabai, and S. Arunkumar, "Dual-band dielectric resonator reflectarray for C/X-bands," *IEEE Antennas Wireless Propag. Lett.*, vol. 11, pp. 1253–1256, 2012.
[13] R. Deng, F. Yang, S. Xu, and M. Li, "Radiation performances of conformal dielectric reflectarray antennas at sub-millimeter waves," in *Proc. IEEE Int. Conf. Microw. Millim. Wave Technol. (ICMMT)*, vol. 1, Jun. 2016, pp. 217–219.
[14] Y. He, Z. Gao, D. Jia, W. Zhang, B. Du, and Z. N. Chen, "Dielectric metamaterial-based impedance-matched elements for broadband reflectarray," *IEEE Trans. Antennas Propag.*, vol. 65, no. 12, pp. 7019–7028, Dec. 2017.
[15] M. Abd-Elhady, W. Hong, and Y. Zhang, "A Ka-band reflectarray implemented with a single-layer perforated dielectric substrate," *IEEE Antennas Wireless Propag. Lett.*, vol. 11, pp. 600–603, 2012.
[16] M. K. T. Al-Nuaimi and W. Hong, "Discrete dielectric reflectarray and lens for E-band with different feed," *IEEE Antennas Wireless Propag. Lett.*, vol. 13, pp. 947–950, 2014.
[17] P. Nayeri, M. Liang, R. A. Sabory-García, M. Tuo, F. Yang, M. Gehm, H. Xin, and A. Z. Elsherbeni, "3D printed dielectric reflectarrays: Low-cost high-gain antennas at sub-millimeter waves," *IEEE Trans. Antennas Propag.*, vol. 62, no. 4, pp. 2000–2008, Apr. 2014.
[18] M. D. Wu, B. Li, Y. Zhou, D. L. Guo, Y. Liu, F. Wei, and X. Lv, "Design and measurement of a 220 GHz wideband 3-D printed dielectric reflectarray," *IEEE Antennas Wireless Propag. Lett.*, vol. 17, no. 11, pp. 2094–2098, Nov. 2018.
[19] A. K. Bhattacharyya, *Phased Array Antennas*. Hoboken, NJ, USA: Wiley, 2006.
[20] *Laird*. [Online]. Available: http://www.lairdtech.com/
[21] M. I. Abbasi, M. H. Dahri, M. H. Jamaluddin, N. Seman, M. R. Kamarudin, and N. H. Sulaiman, "Millimeter wave beam steering reflectarray antenna based on mechanical rotation of array," *IEEE Access*, vol. 7, pp. 145685–145691, 2019.
[22] M. I. Abbasi and M. Y. Ismail, "Reflection loss and bandwidth performance of X-band infinite reflectarrays: Simulations and measurements," *Microw. Opt. Technol. Lett.*, vol. 53, no. 1, pp. 77–80, Jan. 2011.
[23] E.-C. Choi and S. Nam, "W-band low phase sensitivity reflectarray antennas with wideband characteristics considering the effect of angle of incidence," *IEEE Access*, vol. 8, pp. 111064–111073, 2020.
[24] E.-C. Choi and S. Nam, "Analysis and elimination of unwanted resonances for wideband reflectarray antenna design at sub-millimeter waves," *IEEE Access*, vol. 8, pp. 224750–224760, 2020.
[25] S. Zhang, "Three-dimensional printed millimetre wave dielectric resonator reflectarray," *IET Microw., Antennas Propag.*, vol. 11, no. 14, pp. 2005–2009, 2017.
[26] Y.-X. Sun and K. W. Leung, "Millimeter-wave substrate-based dielectric reflectarray," *IEEE Antennas Wireless Propag. Lett.*, vol. 17, no. 12, pp. 2329–2333, Dec. 2018.
[27] W. Li, S. Gao, L. Zhang, Q. Luo, and Y. Cai, "An ultra-wide-band tightly coupled dipole reflectarray antenna," *IEEE Trans. Antennas Propag.*, vol. 66, no. 2, pp. 533–540, Feb. 2018.
[28] S. M. A. M. H. Abadi, K. Ghaemi, and N. Behdad, "Ultra-wideband, true-time-delay reflectarray antennas using ground-plane-backed, miniaturized-element frequency selective surfaces," *IEEE Trans. Antennas Propag.*, vol. 63, no. 2, pp. 534–542, Feb. 2015.

EUN-CHEOL CHOI received the B.S. and M.S. degrees in electronics, telecommunications and computer engineering from Korea Aerospace University, Goyang, in 2012 and 2014, respectively, and the Ph.D. degree in electrical engineering and computer science from Seoul National University, Seoul, South Korea, in 2020.

His research interests include micro-wave and millimeter-wave and reflectarray antenna design and analysis.

SANGWOOK NAM (Senior Member, IEEE) received the B.S. degree in electrical engineering from Seoul National University, Seoul, South Korea, in 1981, the M.S. degree in electrical engineering from the Korea Advanced Institute of Science and Technology (KAIST), Seoul, in 1983, and the Ph.D. degree in electrical engineering from The University of Texas at Austin, Austin, TX, USA, in 1989. From 1983 to 1986, he was a Researcher with the Gold Star Central Research Laboratory, Seoul. Since 1990, he has been a Professor with the School of Electrical Engineering and Computer Science, Seoul National University. His research interests include analysis/design of electromagnetic (EM) structures, antennas, and microwave active/passive circuits.